Available online at website: https://journal.bcrec.id/index.php/jcerp

Journal of Chemical Engineering Research Progress, 3 (2) 2026, 390-399

Original Research Article

# Optimization Studies of The Treatment of Laundry Wastewater Using Activated Carbon Derived from HDPE Chars

**David Emoefe Rockson-Itiveh*, Cyril Oghenekome Anakpoha, Mabel Keke, Marcel Ajogri, Ulakpa Wisdom, Fabian Chidiebere Ozioko, Samson Onoriode Okpo**

*Chemical Engineering Department, Southern Delta University, Ozoro, Nigeria.*

*Received: 26th August 2026; Revised: 6th September 2026; Accepted: 7th September 2026*
*Available online: 10th September 2026; Published regularly: December 2026*

## Abstract

Growing plastic waste and industrial wastewater necessitate sustainable treatment solutions. This study optimized industrial wastewater treatment using activated carbon derived from high-density polyethylene (HDPE) pyrolysis char via thermal activation, eliminating the need for aggressive chemical agents. Characterization via FTIR, BET, and SEM-EDX revealed a micro-mesoporous structure with a BET surface area of 287.3 $m^2/g$, a 90.05 atomic percent carbon content, and dominant pore sizes of 2.1 to 2.6 nm. The adsorbent performance was evaluated against laundry wastewater using a Central Composite Design and Response Surface Methodology. Statistical analysis yielded a robust model ($R^2$ = 0.9406, adequate precision = 15.54) to assess the impact of dosage, contact time, and initial concentration. Numerical optimization identified ideal conditions: 8.68 g/L dosage and 15-minute contact time for a 100 mg/L initial concentration. Experimental validation confirmed a 77.99% total dissolved solids (TDS) reduction, aligning closely with the predicted 79.48%. Post-treatment analysis indicated significant quality improvements, with COD and TOC levels decreasing to 35.8 mg/L and 21.6 mg/L, respectively, while dissolved oxygen increased from 0.6 to 4.3 mg/L. This research confirms that HDPE-derived activated carbon offers an effective, sustainable approach for both wastewater remediation and plastic waste valorization.



***Keywords***: Plastic; HDPE; Pyrolysis; Wastewater; Adsorption; Activated Carbon

***How to Cite***: Rockson-Itiveh, D. E., Anakpoha, C. O., Keke, M., Ajogri, M., Wisdom, U., Ozioko, F., Okpo, S. (2026). Optimization Studies of The Treatment of Laundry Wastewater Using Activated Carbon Derived from HDPE Chars. *Journal of Chemical Engineering Research Progress*, 3 (2), 390-399 (DOI: 10.9767/jcerp.20825)

***Permalink/DOI***: https://doi.org/10.9767/jcerp.20825

## 1. Introduction

Adsorption using activated carbon is widely used in wastewater treatment because of its high surface area, developed pore structure, and ability to remove dissolved organic and inorganic contaminants. However, the relatively high cost of conventional activated carbon can restrict its wider application, particularly where low-cost wastewater-treatment technologies are required. At the same time, the accumulation of post-consumer plastic waste presents an increasing environmental challenge. Thermochemical conversion of plastic waste through pyrolysis produces oil, gas, and a carbon-rich solid char, creating an opportunity to valorize the residual char as an adsorbent rather than treating it as a low-value by-product [1].

Previous studies have investigated activated carbons and carbonaceous adsorbents produced from waste materials for the removal of dissolved solids, dyes, and heavy metals from contaminated water [2]. Plastic pyrolysis chars have also been converted into activated carbons, particularly through chemical activation using agents such as KOH, NaOH, and other activating chemicals, with improvements in surface area and adsorption performance as reported [3]. These studies demonstrate the potential of waste-derived carbonaceous materials for water treatment however, much of the reported work on plastic-

* Corresponding Author.
Email: davidrockyle95@gmail.com (D.E. Rockson-Itiveh)

derived activated carbon has focused on specific contaminants such as heavy metals and has also relied on chemical activation processes [4]. Furthermore, comparatively limited attention has been given to integrating detailed physicochemical characterization of HDPE-derived carbon with statistically optimized treatment of laundry wastewater containing mixtures of dissolved ionic and organic constituents.

This study addresses the research gap arising from the limited understanding of the performance of HDPE pyrolysis char converted into activated carbon without harsh chemical activation for laundry wastewater treatment under statistically optimized conditions. The scientific novelty lies in integrating the valorization of HDPE pyrolysis char, physicochemical characterization using BET, FTIR, SEM and EDX, and response surface optimization of operational treatment variables to establish structure performance relationships for laundry wastewater treatment. This approach provides new experimental evidence connecting the pore structure, surface chemistry and elemental characteristics of HDPE-derived activated carbon with its wastewater-treatment performance, while simultaneously addressing plastic-char valorization and wastewater remediation.

Accordingly, this study aims to prepare activated carbon from HDPE pyrolysis char, characterize its textural, chemical and morphological properties, evaluate its effectiveness in reducing total dissolved solids and improving selected physicochemical characteristics of laundry wastewater, and optimize the adsorption process using central composite design and response surface methodology. The optimized treatment performance is further evaluated by comparing the physicochemical characteristics of the treated wastewater with relevant Nigerian effluent standards.

## 2. Materials and Methods

High-density polyethylene (HDPE) post-consumer plastic waste was sourced, sorted, washed to remove surface dirt, sun-dried, and shredded into flakes of approximately 5-10 mm prior to pyrolysis. All reagents used for the physicochemical analyses of the wastewater (potassium chloride standard solution, buffer solutions of pH 4.0, 7.0 and 9.2, and turbidity standard suspensions) were of analytical grade and were used as received. Nitrogen gas (99.999% purity) was used as the purge/inert gas for the pyrolysis process and as the adsorbate gas during textural characterization. Raw laundry wastewater was obtained directly from a domestic laundering point, collected in clean 25-litre high-density polyethylene containers, and stored at 4°C prior to analysis to minimize microbial degradation of the organic load.

### 2.1. Preparation of Activated Carbon from Plastic Pyrolysis Char

The shredded HDPE flakes were charged into a laboratory-scale batch pyrolysis reactor and heated under a limited-oxygen (inert nitrogen-purged) atmosphere to convert the polymer into gaseous, liquid, and solid (char) fractions. Pyrolysis proceeded through slow de-volatilisation of the polymer chains, releasing condensable oil vapours and non-condensable gases, and leaving behind a carbon-rich solid residue (char). The resulting HDPE-derived biochar was allowed to cool under an inert atmosphere to room temperature, after which it was pulverised and sieved to a uniform particle size.

#### 2.1.1. Char activation

The pyrolysis char was activated to develop the porosity and surface area required for an effective adsorbent. Activation was carried out to promote the release of volatile matter trapped within the carbon matrix and to open the pore network. After activation, the resulting activated carbon was cooled, ground, and sieved to a particle size of 0.24 g. The sample was subsequently used for textural analysis, while separate batches were reserved for the wastewater adsorption trials.

### 2.2. Collection and Physicochemical Characterization of Laundry Wastewater

Composite laundry wastewater samples were characterised for pH, electrical conductivity (EC), turbidity, dissolved oxygen (DO), total organic compound (TOC), total dissolved solids (TDS), and chemical oxygen demand (COD) before and after adsorption treatment, using the following standardised methods.

### 2.3. Batch Adsorption Experiments

Batch adsorption tests were conducted by contacting pre-weighed masses of the HDPE-derived activated carbon with fixed volumes of raw laundry wastewater under agitation at room temperature. The three operational variables investigated were the adsorbent dosage (A), varied between 1.0 and 10.0 g/L, the contact time (B), varied between 15 and 120 minutes and initial concentration (C) varied between 10 to 130.68 mg/L. At the end of each contact period, the suspension was filtered, and the residual TDS concentration of the filtrate was measured. The

percentage TDS reduction achieved in each run was computed relative to the TDS of the untreated wastewater.

### 2.4. Experimental Design and Statistical Optimization

The effects of adsorbent dosage, contact time, and initial concentration on the percentage reduction in TDS were investigated and optimized using response surface methodology (RSM) based on a central composite design (CCD). A rotatable, randomised, three factor CCD (Design-Expert, quadratic response-surface model, 19 experimental runs, no blocking) was constructed with adsorbent dosage (A), contact time (B) and (C) Initial Concentration as the independent factors and percentage TDS reduction as the response. The coded and actual levels of the factors are summarized in Table 1.

## 3. Results and Discussion

### 3.1. Textural Properties of the Activated Carbon Derived from HDPE Pyrolysis Char

Nitrogen adsorption–desorption analysis showed that the activated carbon derived from HDPE pyrolysis char exhibited excellent BET linearity ($r$ = 0.999512) over 0.058–0.303 $P/P_0$ (Figure 1). The multi-point BET surface area was 287.252 m²/g, compared with 270.9 m²/g for the single-point BET method, while the Langmuir surface area was 483.729 m²/g. The relatively high surface area indicates the development of an accessible porous structure, demonstrating the material's potential as an adsorbent for industrial wastewater treatment [5].

The surface-area estimates followed the order Langmuir > BJH > DH > multi-point BET > single-point BET > DR-micropore > DFT, reflecting differences in the pore fractions captured by each model. The multi-point BET surface area of 287 m²/g falls within the reported range for plastic-waste-derived activated carbons and is comparable to physically activated plastic char, although lower than values reported for strongly KOH-activated carbons [6]. The pore-volume and pore-diameter analysis provides further insight into the porous architecture of the material. The Dubinin-Astakhov (DA) micropore analysis (Figure 2) resolved a dominant narrow pore-size population with a modal diameter of 2.140 nm and a best fit at an adsorption-energy parameter $E$ of 1.832 kJ/mol ($n$ = 1.000), giving a total DA micropore volume of 0.203 cc/g. This indicates that the porosity of the activated carbon is concentrated principally in the upper-micropore/lower-mesopore range (around 2 nm), a

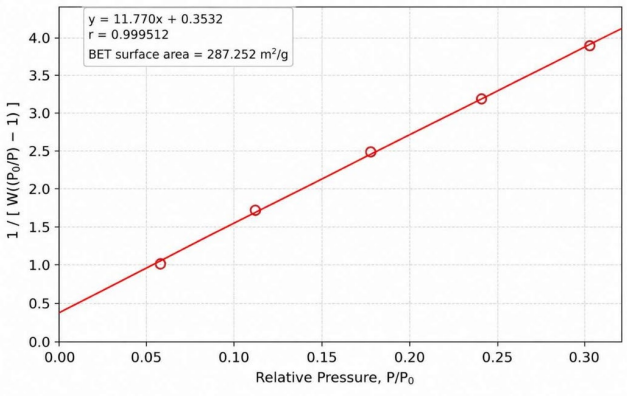


Figure 1. Multi-point BET transform plot of the HDPE-derived activated carbon ($N_2$, 77.350 K); the linear fit (slope = 11.770, intercept = 0.3532, $r$ = 0.999512) yields a BET surface area of 287.252 m²/g.

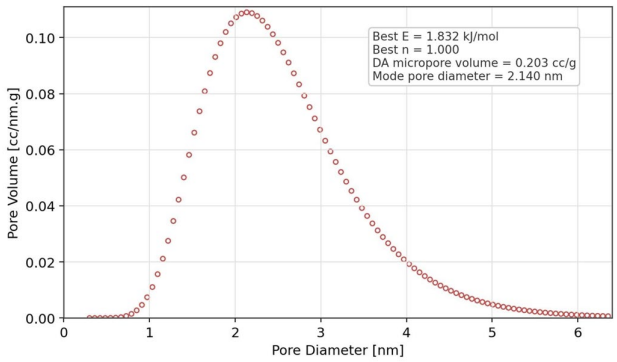


Figure 2. DA-method micropore size distribution [$dV(d)$ versus pore diameter] of the HDPEderived activated carbon, showing a dominant pore population centred at 2.14 nm (DA micropore volume = 0.203 cm³/g).

Table 1. Coded and actual levels of the experimental design factors (rotatable central composite design, α = 1.414).

| Factor | Minimum (actual) | Maximum (actual) | Coded low (-1) | Coded high (+1) | Mean |
|---|---|---|---|---|---|
| A: Adsorbent dosage (g/L) | 1.00 | 10.00 | 2.32 | 8.68 | 5.50 |
| B: Time (minutes) | 15.00 | 120.00 | 30.38 | 104.62 | 67.50 |
| C: Initial Concentration (mg/L) | 10 | 130.68 | 10 | 100 | 57.18 |

size class of relevance to the entrapment of small dissolved ionic and organic species that contribute to TDS and COD in laundry effluents [7].

The BJH adsorption dV(d) analysis (Figure 3), evaluated over the narrower 1.481-2.434 nm window resolved by the instrument's tabulated interval, gave a cumulative BJH pore volume of 0.140 cc/g, a BJH surface area of 290.4 $m^2/g$, and a modal (Dv(d)) pore diameter of 2.108 nm, essentially coincident with the DA-derived mode. The close agreement between the DA, BJH, and DH modal pore diameters (2.108-2.140 nm) is consistent with the H3-type hysteresis behaviour reported for flaky, non-rigid aggregate morphologies typical of pyrolysis chars [6].

The DR method yielded a micropore width of 3.866 nm, micropore volume of 0.146 $cm^3/g$, adsorption energy of 6.725 kJ/mol, and apparent micropore surface area of 409.8 $m^2/g$. In contrast, NLDFT analysis gave lower values of 161.8 $m^2/g$ for cumulative surface area and 0.128 $cm^3/g$ for pore volume, with a modal pore width of 2.647 nm and a low fitting error of 1.057%. The differences among DR, DA/BJH, and NLDFT estimates reflect the distinct assumptions underlying these pore-structure models, particularly for heterogeneous and disordered carbon materials.

### 3.2. Surface Functional-Group Chemistry (FTIR)

The FTIR spectrum of the HDPE pyrolysis char (Figure 4) exhibited four prominent absorption bands at 3413.89, 1635.15, 1451.48, and 875.52 $cm^{-1}$. The broad band at 3413.89 $cm^{-1}$ was attributed to O–H stretching vibrations associated with surface hydroxyl groups and adsorbed moisture, indicating the presence of oxygen-containing surface functionalities [7]. The band at 1635.15 $cm^{-1}$ was assigned primarily to aromatic C=C skeletal vibrations, with possible contributions from C=O groups formed during thermal degradation. The absorption at 1451.48 $cm^{-1}$ corresponded to C–H bending vibrations of residual aliphatic and methylene groups. Meanwhile, the intense band at 875.52 $cm^{-1}$ was associated with out-of-plane aromatic C–H bending, suggesting the development of condensed aromatic structures during pyrolysis.

The presence of these functional groups indicates that pyrolysis transformed the HDPE polymer matrix into a carbon-rich material containing both aromatic and oxygen-containing surface functionalities. Such functional groups can contribute to interactions between the char surface and wastewater contaminants through mechanisms such as hydrogen bonding, π–π interactions, and surface complexation. Therefore, the FTIR results support the potential suitability of the HDPE-derived pyrolysis char as an adsorbent for wastewater treatment.

### 3.3. Surface Morphology of the HDPE Pyrolysis Char

Figure 5 shows the SEM micrograph of the HDPE pyrolysis char at 1500× magnification. The char exhibited an irregular and heterogeneous morphology, characterized by agglomerated

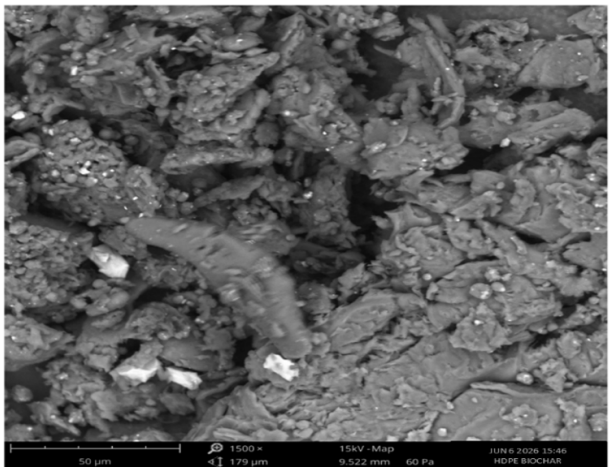


Figure 5. Surface morphology of the HDPE Pyrolysis Char.

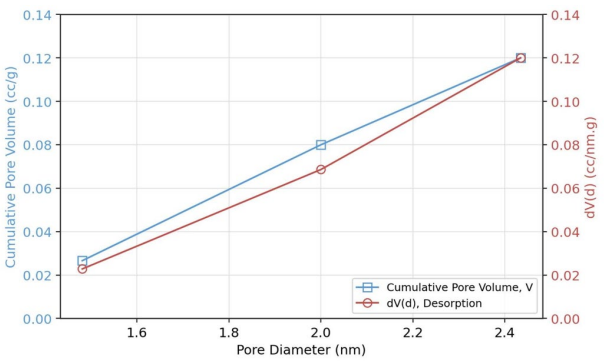


Figure 3. BJH adsorption cumulative pore volume, $V$, and pore-volume derivative, $dV(d)$, as a function of pore diameter for the HDPE-derived activated carbon.

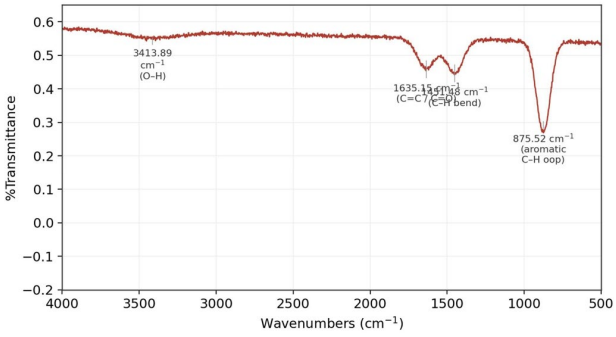


Figure 4. FTIR spectrum of the HDPE-derived pyrolysis char, with the four dominant absorption bands identified by the automated peak-search routine (absolute threshold 0.337, sensitivity 50) labelled and tentatively assigned.

particles, rough surfaces, folds, fractures, cracks, and visible cavities. These features indicate substantial structural modification of the HDPE during pyrolysis, likely resulting from polymer decomposition and the release of volatile products. The resulting cracks and voids may provide pathways for the penetration of activating agents and facilitate the development of additional porosity during activation.

Dark regions observed between the particles may represent surface cavities, fissures, or interparticle voids that could contribute to adsorption [8]. However, these features cannot be directly classified as micropores because micropores are smaller than 2 nm and cannot be reliably resolved at the applied magnification. Thus, the SEM primarily provides information on external morphology, whereas the BET analysis offers more reliable evidence of the internal surface area and pore structure. Bright particles observed in some regions may be associated with inorganic residues, additives, mineral fillers, or impurities from the HDPE feedstock.

Table 2. EDX elemental composition (atomic and weight percentage) of the HDPEderived pyrolysis char surface (field of view 537 μm, 15 kV, BSD-Full detector).

| Element | Symbol | Atomic Conc. (%) | Weight Conc. (%) |
|---|---|---|---|
| Carbon | C | 90.05 | 76.31 |
| Calcium | Ca | 1.36 | 3.84 |
| Potassium | K | 1.38 | 3.80 |
| Silicon | Si | 1.38 | 2.74 |
| Fluorine | F | 1.68 | 2.25 |
| Iron | Fe | 0.49 | 1.92 |
| Phosphorus | P | 0.87 | 1.90 |
| Aluminium | Al | 0.91 | 1.74 |
| Magnesium | Mg | 0.65 | 1.12 |

### 3.4. Energy-Dispersive X-Ray Spectroscopy (EDX)

The corresponding EDX elemental map (Table 2) confirmed that carbon was overwhelmingly the dominant element, accounting for 90.05 atomic % (76.31 weight %) of the analysed region, consistent with a carbon-rich pyrolysis char. The remaining composition comprised a range of minor and trace inorganic elements, principally calcium (3.84 wt.%), potassium (3.80 wt.%), zinc (3.00 wt.%), silicon (2.74 wt.%), fluorine (2.25 wt.%), iron (1.92 wt.%), phosphorus (1.90 wt.%), aluminium (1.74 wt.%), magnesium (1.12 wt.%), chlorine (0.86 wt.%) and sulphur (0.52 wt.%). The remaining measurable composition comprised calcium (3.84 wt.%), potassium (3.80 wt.%), silicon (2.74 wt.%), fluorine (2.25 wt.%), iron (1.92 wt.%), phosphorus (1.90 wt.%), aluminium (1.74 wt.%), and magnesium (1.12 wt.%). The presence of these inorganic constituents may be associated with additives, fillers, pigments, or impurities present in the post-consumer HDPE feedstock [9].

### 3.5. Response Surface Optimization of the Adsorption Process

#### 3.5.1. Experimental design matrix

Table 3 presents the central composite design comprising 19 experimental runs with variations in adsorbent dosage, contact time, and

Table 3. Central Composite Design matrix and experimental results for percentage TDS reduction as a function of adsorbent dosage (A), contact time (B) and Initial Concentration.

| Std | Run | Factor 1 A: Adsorbent dosage (g/L) | Factor 2 B: Time (min) | Factor 3 C: Initial Concentration (mg/L) | Response 1 TDS Reduction (%) |
|---|---|---|---|---|---|
| 8 | 1 | 8.68198 | 104.623 | 100 | 25.6 |
| 19 | 2 | 4.84099 | 59.8115 | 55 | 49.3 |
| 10 | 3 | 11.3007 | 59.8115 | 55 | 48.87 |
| 15 | 4 | 4.84099 | 59.8115 | 55 | 49.33 |
| 13 | 5 | 4.84099 | 59.8115 | 20.6807 | 66.44 |
| 18 | 6 | 4.84099 | 59.8115 | 55 | 59.3 |
| 12 | 7 | 4.84099 | 135.175 | 55 | 34.49 |
| 2 | 8 | 8.68198 | 15 | 10 | 43.96 |
| 16 | 9 | 4.84099 | 59.8115 | 55 | 49.3 |
| 3 | 10 | 1 | 104.623 | 10 | 77.55 |
| 17 | 11 | 4.84099 | 59.8115 | 55 | 49.3 |
| 4 | 12 | 8.68198 | 104.623 | 10 | 48.49 |
| 5 | 13 | 1 | 15 | 100 | 52.75 |
| 9 | 14 | 1.61876 | 59.8115 | 55 | 49.73 |
| 1 | 15 | 1 | 15 | 10 | 44.48 |
| 6 | 16 | 8.68198 | 15 | 100 | 77.99 |
| 7 | 17 | 1 | 104.623 | 100 | 25.76 |
| 14 | 18 | 4.84099 | 59.8115 | 130.681 | 42.97 |
| 11 | 19 | 4.84099 | 15.5522 | 55 | 57.11 |

initial pollutant concentration. TDS reduction ranged from 25.60% to 77.99%**,** with the highest reduction recorded in Run 16 and the lowest in Run 1. The variation in responses indicates possible interactions among the process variables, supporting the use of a quadratic response-surface model to evaluate their individual, interactive, and nonlinear effects and determine the optimum treatment conditions [10].

3.5.2. Analysis of Variance for the Quadratic Model of TDS Reduction

The ANOVA results (Table 4) showed that the quadratic model for TDS reduction was statistically significant ($F = 15.83$, $p = 0.0002$). Among the linear terms, contact time (B) and initial concentration (C) significantly influenced TDS reduction ($p < 0.05$), whereas the linear effect of adsorbent dosage (A) was not significant ($p = 0.8487$). The interaction terms AB and AC were significant ($p = 0.0033$ and $p = 0.0030$, respectively), while BC exhibited the strongest interaction effect ($F = 73.99$, $p < 0.0001$). The quadratic terms $A^2$, $B^2$ and $C^2$ were not statistically significant within the investigated experimental range ($p > 0.05$). The lack of fit was not significant ($F = 1.28$, $p = 0.4161$), indicating no statistically significant evidence of model inadequacy relative to the pure experimental error. Overall, the results demonstrate that contact time, initial concentration and factor interactions, particularly the interaction between contact time and initial concentration, played important roles in determining TDS reduction.

3.5.3. Fit statistics for the TDS reduction model

The model-fit statistics for TDS reduction are presented in Table 5. The model recorded an $R^2$ value of 0.9406, indicating that approximately 94.06% of the variation in TDS reduction was explained by changes in the operational parameters investigated. Only 5.94% of the observed variation remained unexplained by the fit model. This demonstrates a strong relationship between experimental factors and TDS reduction.

The model showed good predictive performance, with an adjusted $R^2$ of 0.8812 and predicted $R^2$ of 0.7755, indicating that the model explained a substantial proportion of the variation in TDS reduction and had reasonable predictive capability. The difference between the two values **(**0.1057**)** was below the recommended 0.20, confirming good agreement between model fitting and prediction. The standard deviation (4.81) and coefficient of variation (9.59%) indicated relatively low experimental variability, while the adequate precision of 15.5378, well above the recommended value of 4, demonstrated a strong signal-to-noise ratio. Overall, the model adequately represented the experimental data and was suitable for prediction and optimization within the investigated operating ranges.

3.5.4. Effect of adsorbent dosage and time on TDS reduction

The three-dimensional response surface (Figure 6) demonstrated that adsorbent dosage and contact time jointly influenced TDS

Table 5. Fit statistics for the quadratic RSM model of percentage TDS reduction.

| | | | |
|---|---|---|---|
| Std. Dev. | 4.81 | $R^2$ | 0.9406 |
| Mean | 50.14 | Adjusted $R^2$ | 0.8812 |
| C.V. % | 9.59 | Predicted $R^2$ | 0.7755 |
| | | Adeq Precision | 15.5378 |

Table 4. ANOVA for the quadratic response-surface model fitted to percentage TDS reduction.

| Source | Sum of Squares | df | Mean Square | F-value | p-value | |
|---|---|---|---|---|---|---|
| Model | 3294.27 | 9 | 366.03 | 15.83 | 0.0002 | significant |
| A-Adsorbent dosage | 0.8918 | 1 | 0.8918 | 0.0386 | 0.8487 | |
| B-Time | 331.96 | 1 | 331.96 | 14.36 | 0.0043 | |
| C-Initial Concentration | 285.27 | 1 | 285.27 | 12.34 | 0.0066 | |
| AB | 363.69 | 1 | 363.69 | 15.73 | 0.0033 | |
| AC | 373.46 | 1 | 373.46 | 16.15 | 0.0030 | |
| BC | 1710.54 | 1 | 1710.54 | 73.99 | < 0.0001 | |
| $A^2$ | 11.11 | 1 | 11.11 | 0.4807 | 0.5056 | |
| $B^2$ | 60.88 | 1 | 60.88 | 2.63 | 0.1391 | |
| $C^2$ | 3.46 | 1 | 3.46 | 0.1499 | 0.7077 | |
| Residual | 208.08 | 9 | 23.12 | | | |
| Lack of Fit | 128.20 | 5 | 25.64 | 1.28 | 0.4161 | not significant |
| Pure Error | 79.88 | 4 | 19.97 | | | |
| Cor Total | 3502.35 | 18 | | | | |

reduction. TDS removal increased from approximately 40–45% at low dosage (1–3 g/L) and short contact time (15–40 min) to about 60–65% at higher dosage (6–8 g/L) and extended contact time (>80 min). The improvement with increasing dosage may be attributed to the greater availability of adsorption sites, while longer contact time facilitates mass transfer and diffusion of dissolved species into the adsorbent pores [11]. The gradual flattening of the surface at longer contact times suggests that adsorption equilibrium was approached, limiting further improvement [12]. The curvature of the surface confirms an interactive, nonlinear relationship between the variables. These findings demonstrate the importance of simultaneous optimization of dosage and contact time for efficient TDS removal while minimizing unnecessary adsorbent use and treatment duration.

### 3.5.5. Effect of adsorbent dosage and initial concentration on TDS reduction

The response surface plot illustrates the combined effects of adsorbent dosage (A) and initial concentration (C) on TDS reduction (Figure 7). Increasing adsorbent dosage enhanced TDS removal, likely due to the increased availability of active adsorption sites and surface area [13]. In contrast, higher initial concentration slightly reduced removal efficiency, probably because of increased competition among dissolved species for limited adsorption sites and progressive surface saturation. The negative effect of concentration was partly offset by increasing the adsorbent dosage, which provided additional sites for contaminant uptake [14]. Overall, the response surface indicates that higher adsorbent dosage combined with low-to-moderate initial concentration favours improved TDS reduction, highlighting the importance of optimizing dosage according to wastewater characteristics for efficient treatment.

### 3.5.6. Effect of contact time and initial concentration on TDS reduction

The response surface plot demonstrates the interactive effects of initial concentration (C) and contact time (B) on TDS reduction (Figure 8). TDS removal increased with increasing contact time

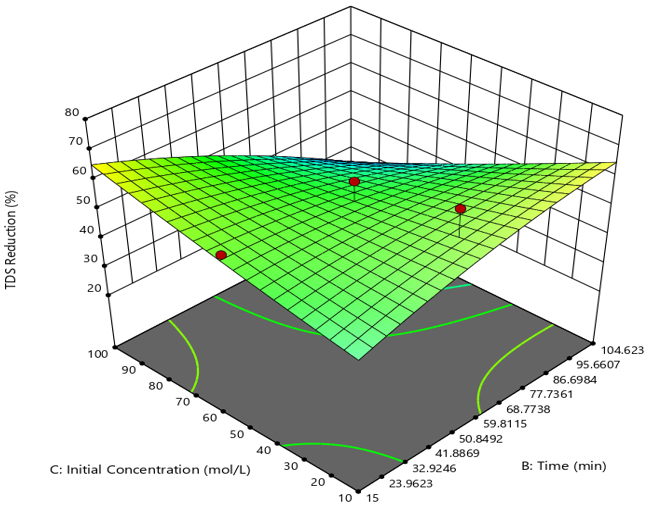


Figure 8. Three-dimensional response surface showing the combined effect of initial concentration (C) and Time (B) on percentage TDS reduction.

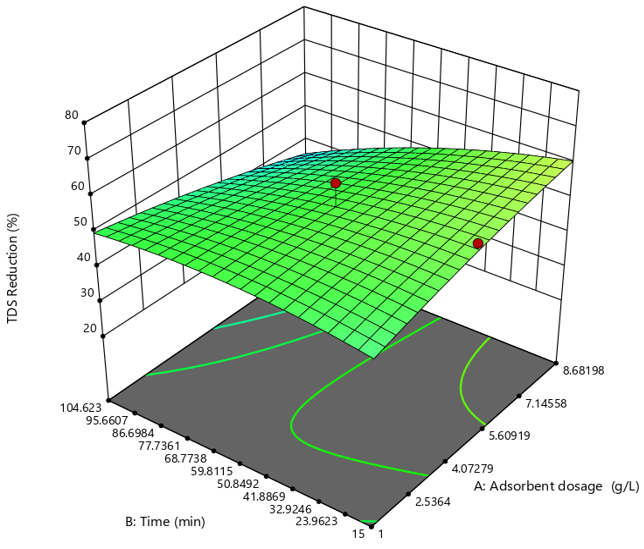


Figure 6. Three-dimensional response surface showing the combined effect of adsorbent dosage (A) and contact time (B) on percentage TDS reduction.

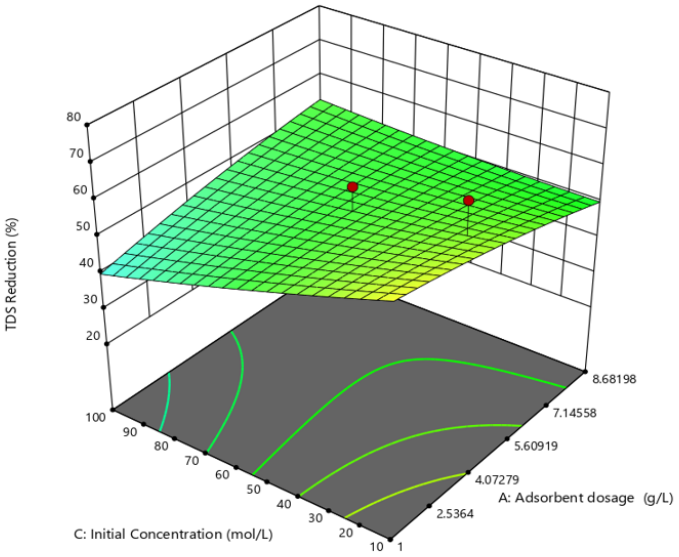


Figure 7. Three-dimensional response surface showing the combined effect of adsorbent dosage (A) and initial concentration (C) on percentage TDS reduction.

but decreased slightly at higher initial concentrations. The positive effect of contact time is attributed to enhanced diffusion of dissolved species into the adsorbent pores and increased interaction with available active sites until equilibrium is approached [15]. Conversely, higher initial concentration increases competition for limited adsorption sites, resulting in lower percentage removal.

3.5.7. Model validation: predicted versus actual TDS reduction

The predicted versus actual plot (Figure 9) showed good agreement between the experimental and model-predicted TDS removal values, with most points closely distributed around the diagonal line. The model exhibited strong reliability, with an $R^2$ of 0.9406, indicating that 94.06% of the variation in TDS reduction was explained by the model. The adjusted $R^2$ (0.8812) and predicted $R^2$ (0.7755) also demonstrated reasonable predictive performance. Furthermore, the adequate precision of 15.5378, exceeding the recommended value of 4, confirmed an adequate signal, while the coefficient of variation of 9.59% indicated acceptable experimental precision. Overall, the close agreement between predicted and actual values confirms that the developed CCD model is reliable for predicting and optimizing TDS removal within the experimental range, consistent with model validation approaches reported in adsorption optimization studies using RSM [16].

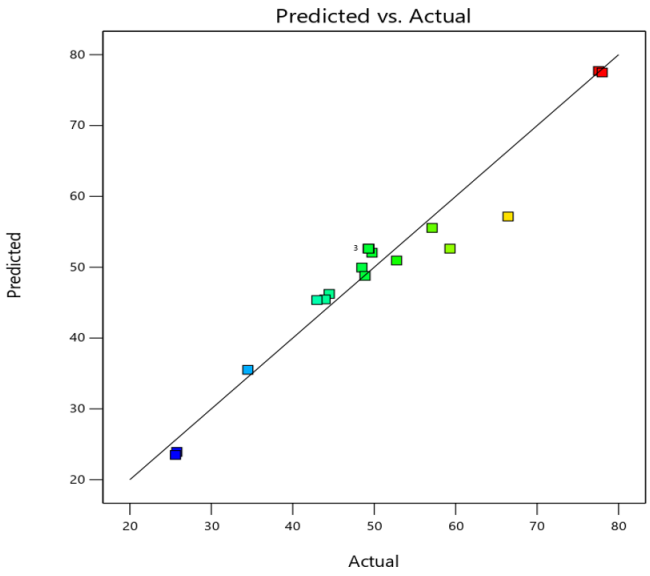


Figure 9. Parity plot of predicted versus actual TDS removal.

3.6. Comparison of Physicochemical Characteristics of Treated Laundry Wastewater with Nigerian Effluent Standards and Evaluation of HDPE Char Treatment Performance

Table 6 compares the physicochemical characteristics of the treated laundry wastewater with NESREA (2011) and FEPA effluent standards. The treatment process using activated carbon derived from HDPE pyrolysis char resulted in substantial improvement in wastewater quality. The treated wastewater recorded a pH of 7.4**,** which falls within the acceptable limits of both NESREA (6.5–8.5) and FEPA (6.0–9.0), indicating that the adsorbent treatment maintained a suitable chemical condition. The reduction in TDS from 430 ppm (untreated wastewater) to 73 ppm after treatment, together with the decrease in electrical conductivity and salinity, demonstrates the ability of HDPE-derived activated carbon to remove dissolved ionic substances from the wastewater [17]. Similarly, the increase in dissolved oxygen from 0.6 mg/L to 4.3 mg/L indicates reduced organic pollution and improved wastewater quality after adsorption treatment. The considerable reduction in COD from 129.6 mg/L to 35.8 mg/L and TOC to 21.6 mg/L further confirms the effectiveness of HDPE pyrolysis char-derived activated carbon in removing organic contaminants [18]. This performance can be attributed to the porous structure and available surface functional groups of activated carbon, which facilitate adsorption of organic molecules

Table 6. Comparison of characteristics of the treated laundry wastewater with the limits prescribed by the National Environmental (Surface and Groundwater Quality Control) Regulations, 2011 and the FEPA effluent limitation guidelines.

| Property | Final value | NESREA Standard (2011) | FEPA Effluent Limit |
|---|---|---|---|
| pH | 7.4 | 6.5 – 8.5 | 6.0 – 9.0 |
| Total Dissolved Solids, TDS (ppm) | 73 | Not specified | 2,000 |
| Electrical Conductivity, EC (µS/cm) | 146 | Not specified | Not specified |
| Dissolved Oxygen, DO (mg/L) | 4.3 | ≥ 4.0 | Not specified |
| Salinity (ppt) | 0.17 | N`ot specified | Not specified |
| Chemical Oxygen Demand, COD (mg/L) | 35.8 | ≤ 30 | Not specified |
| Total Organic Compound, TOC (mg/L) | 21.6 | Not specified | Not specified |

through surface interactions and pore diffusion mechanisms [19]. Similar improvements in wastewater treatment using biomass- and waste-derived activated carbons have been reported due to their high surface area and adsorption capacity [20].

## 4. Conclusion

This study successfully evaluated and optimized the treatment of laundry wastewater using activated carbon derived from HDPE pyrolysis char. Characterization of the adsorbent confirmed the development of a porous, carbon-rich material, with a BET surface area of 287.252 $m^2/g$, dominant pore sizes around 2.1–2.6 nm, and carbon accounting for 90.05 atomic % of the analysed surface. FTIR and SEM analyses further confirmed the presence of surface functional groups and an irregular porous morphology suitable for adsorption. The response surface methodology demonstrated that the investigated operating conditions significantly influenced TDS reduction and provided a statistically adequate model for process optimization. The model achieved $R^2$ = 0.9406, adjusted $R^2$ = 0.8812, predicted $R^2$ = 0.7755, and adequate precision = 15.5378. Under the investigated conditions, a maximum experimental TDS reduction of 77.99% was obtained. Treatment also improved the physicochemical quality of the laundry wastewater, reducing TDS from 430 to 73 mg/L and COD from 129.6 to 35.8 mg/L, while dissolved oxygen increased from 0.6 to 4.3 mg/L. The treated wastewater attained acceptable values for several evaluated parameters, although the final COD remained slightly above the NESREA limit of 30 mg/L. Therefore, activated carbon derived from HDPE pyrolysis char demonstrated potential as an adsorbent for the optimized treatment of laundry wastewater, providing a pathway for simultaneous valorization of plastic pyrolysis char and improvement of wastewater quality.

## Acknowledgment

Our kind appreciation goes to the Chemical Engineering Department Laboratory technologist for their patience and hard work throughout this research.

## CRedit Authors Statement

Author Contributions: Rockson-Itiveh D.E: Conceptualization, Methodology, Investigation, Resources, Data Curation, Writing, Review and Editing, Supervision; Anakpoha O.C: Conceptualization, Methodology, Formal Analysis, Data Curation, Writting Draft Preparation, Visualization, Software, Project Administration; Mabel Keke, Writing, Review and Editing, Data Curation; Marcel Ajogri: Investigation, Resources, Writing, Review and Editing, Validation. All authors have read and agreed to the published version of the manuscript.

## References

[1] Ani, J.U., Okoro, U.C., Aneke, L.E., Onukwuli, O.D., Obi, I.O., Akpomie, K.G., Ofomatah, A.C. (2019). Application of response surface methodology for optimization of dissolved solids adsorption by activated coal. *Applied Water Science*, 9, 60. DOI: 10.1007/s13201-019-0943-7.

[2] Verma, R., Choudhary, M. (2025). Sustainable valorization of plastic waste into activation char through pyrolysis. *International Journal of Environmental Health Researc*h, 35(10), 3133–3145. DOI: 10.1080/09603123.2025.2474093.

[3] Mustafa, M., Epelle, E.I., Macfarlane, A., Cusack, M., Burns, A., Yaseen, M. (2025). Innovative approaches to greywater micropollutant removal: AI-driven solutions and future outlook. *RSC Advances*, 15, 12125–12151. DOI: 10.1039/D5RA00489F.

[4] Ahangar, F.A., Rashid, U., Ahmad, J., Tsubota, T., Alsalme, A. (2021). Conversion of waste polyethylene terephthalate (PET) polymer into activated carbon and its feasibility to produce green fuel. *Polymers*, 13(22), 3952. DOI: 10.3390/polym13223952.

[5] Nicholas, H.L., Mabbett, I., Apsey, H., Robertson, I. (2022). Physico-chemical properties of waste derived biochar from community scale faecal sludge treatment plants. *Gates Open Research*, 6, 96. DOI: 10.12688/gatesopenres.13727.2.

[6] Solís, R.R., Martín-Lara, M.Á., Ligero, A., Balbís, J., Blázquez, G., Calero, M. (2022). Revalorizing a pyrolytic char residue from post-consumer plastics into activated carbon for the adsorption of lead in water. *Applied Sciences*, 12(16), 8032. DOI: 10.3390/app12168032.

[7] Rockson-Itiveh, D., Chidiebere, F., Keke, M. (2024). The use of chitosan as a coagulant in wastewater treatment. *International Journal of Environmental Pollution and Environmental Modelling*, 7(1), 27–36. https://izlik.org/JA85SR65JU.

[8] Pereira, L., Castillo, V., Calero, M., Blázquez, G., Solís, R.R., Martín-Lara, M.Á. (2024). Insights into using plastic waste to produce activated carbons for wastewater treatment applications: A review. *Journal of Water Process Engineering*, 62, 105386. DOI: 10.1016/j.jwpe.2024.105386.

[9] Pereira, L., Castillo, V., Calero, M., Blázquez, G., Solís, R.R., Martín-Lara, M.Á. (2024). Conversion of char from pyrolysis of plastic wastes into alternative activated carbons for heavy metal removal. *Environmental Research*, 250, 118558. DOI: 10.1016/j.envres.2024.118558.

[10] Thommes, M., Kaneko, K., Neimark, A.V., Olivier, J.P., Rodriguez-Reinoso, F., Rouquerol, J., Sing, K.S.W. (2015). Physisorption of gases, with special reference to the evaluation of surface area and pore size distribution (IUPAC Technical Report). *Pure and Applied Chemistry*, 87(9–10), 1051–1069. DOI: 10.1515/pac-2014-1117.

[11] La, D.D. (2024). High porous activated carbon from plastic waste using direct chemical activation for the treatment of organic dyes in water. *International Journal of Science and Research*, 13(3), 1241–1246. DOI: 10.21275/SR24320174833.

[12] Barracco, F., Parisi, E., Pipitone, G., Simone, E., Bensaid, S., Fino, D. (2024). Valorization of pyrolytic plastic-derived char for adsorption of wastewater contaminants: A kinetic and thermodynamic investigation. *International Journal of Environmental Science and Technology*, 21, 6513–6530. DOI: 10.1007/s13762-024-05467-1.

[13] Bhattacharya, R. (2023). A review on production and application of activated carbon from discarded plastics in the context of 'waste treats waste'. *Journal of Environmental Management*, 325, 116613. DOI: 10.1016/j.jenvman.2022.116613.

[14] García Ávila, F., Cabrera-Sumba, J., Valdez-Pilataxi, S., Villalta-Chungata, J., Valdiviezo-Gonzales, L., Alegria-Arnedo, C. (2025). Removal of heavy metals in industrial wastewater using adsorption technology: Efficiency and influencing factors. *Cleaner Engineering and Technology*, 24, 100879. DOI: 10.1016/j.clet.2025.100879.

[15] Federal Republic of Nigeria. (2011). National Environmental (Surface and Groundwater Quality Control) Regulations, S.I. No. 22 of 2011. Federal Republic of Nigeria Official Gazette, 98(49), B693–B728.

[16] National Environmental Standards and Regulations Enforcement Agency. (n.d.). Laws and regulations: National Environmental (Surface and Groundwater Quality Control) Regulations, S.I. No. 22 of 2011.

[17] Tadess, N.D., Gezahegn, G.Y., Abrha, Y.H. (2025). Adsorption of TDS and chloride ions from partially treated tannery wastewater using activated coffee husk. *Discover Materials*, 5, 8. DOI: 10.1007/s43939-025-00177-y.

[18] Hashemi, S.H., Soleimani, M. (2025). Usage of magnetic activated carbon as a potential adsorbent for aniline adsorption from wastewater. *Scientific Reports*, 15, 4570. DOI: 10.1038/s41598-025-89129-3.

[19] Rockson-Itiveh, D.E., Keke, M., Ozioko, F.C., Otuya, I.C. (2023). Bentonite clay as an alternative adsorbent for removal of heavy metals in wastewater. *FUOYE Journal of Engineering and Technology*, 8(3), 360–364. DOI: 10.46792/fuoyejet.v8i3.1033.

[20] Uyigue, L., Rockson-Itiveh, D. (2021). Evaluation of proposed treatment process for abattoir wastewater. *International Journal of Innovative Science and Research Technology*, 6(4), 1038–1043.